



# Preparation, characterization and utilization of (Ni:Cu) bimetallic system loaded on zeolites

Islam Hamdy Abd El Maksod<sup>a,c</sup>, Tamer S. Saleh<sup>b</sup>, Eman Z. Hegazy<sup>a,c,\*</sup>

<sup>a</sup> Chemistry Department, Faculty of Science, King Abdulaziz University, Saudi Arabia

<sup>b</sup> Green Chemistry department, National Research Centre, Dokki, El Behouth Street, Dokki, Cairo, Egypt

<sup>c</sup> Physical Chemistry department, National Research Centre Dokki, El Behouth Street, Dokki, Cairo, Egypt

## ARTICLE INFO

### Article history:

Received 18 May 2010

Received in revised form 13 July 2010

Accepted 14 July 2010

Available online 21 July 2010

### Keywords:

Bimetallic system

Zeolites

Egyptian kaolin

Hydrogenation reaction

XRD

ESR

TEM

## ABSTRACT

Preparation and characterization of bimetallic system (Ni:Cu) loaded on zeolites were performed and examined in hydrogenation process for *p*-nitrophenol into *p*-aminophenol. Two types of zeolites were used as supports for bimetallic system namely LTA and FAU originally prepared from Egyptian kaolin ore. Several techniques were employed for the characterization of prepared catalysts including XRD, ESR, TEM and measurements of catalytic activity. The bimetallic catalyst showed superior catalytic activity in a system used hydrazine hydrate as hydrogen donor. The results showed that catalyst supported on LTA zeolite is being more effective than that supported on FAU. The reaction proceeds to 100% conversions through only few seconds.

© 2010 Elsevier B.V. All rights reserved.

## 1. Introduction

The preparation of the catalyst is an important issue for many recent researches for many applications [1–6].

The nickel metal catalyst is widely employed in many fields for hydrogenation process [7–14]. The hydrogenation process is considered to be a vital process for many industrial applications such as hydrogenation of edible oil [13,14].

The use of bimetallic system as a catalyst is recently attracted more interest not only due to the highly synergetic effect of bimetallic systems but also due to the change in the physical properties of the resulted alloy which affects mainly the stability and the durability of the catalysts [15–24].

The reduction of these alloys is another issue of challenging, thus many papers use high pressure hydrogen and high temperature in hydrogenation process [25–29]. The use of chemical method reduction is also reported [30].

Many analgesic and antipyretic drugs, such as paracetamol, acetanilide, phentacin, etc depend mainly on *p*-aminophenol as intermediate [31–37] besides its use in chemical dye industries [32–38].

The preparation of *p*-aminophenol from *p*-nitrophenol could be achieved by many cited methods such as: (1) metal/acid reduction [39], (2) catalytic hydrogenation [40], (3) electrolytic reduction [41], (4) homogeneous catalytic transfer hydrogenation [42], and (5) heterogeneous catalytic transfer hydrogenation, etc.

The direct catalytic hydrogenation of *p*-nitrophenol into *p*-aminophenol was proved to be the most effective method which was proved by our previous work to use nickel catalyst supported on SiO<sub>2</sub> or Al<sub>2</sub>O<sub>3</sub> [43] or a mixture of both [43,44]. In our previous work [43,44], the use of hydrazine hydrate as hydrogen donor was proved to be very effective and green route for the process. The present work aims at the study of the effect of crystalline aluminosilicates such as zeolites in the same system using single nickel metal or bimetallic Ni/Cu system.

The zeolites employed are LTA and FAU which have been prepared from Egyptian kaolin [13,14]. The use of Egyptian kaolin as primary source in the preparation of zeolites drive more economic impact for this work due to the high availability of kaolin resources in many countries and its very cheap price.

## 2. Experimental

### 2.1. Materials

The chemicals employed are, Egyptian kaolin containing mainly, 53% SiO<sub>2</sub> and 32% Al<sub>2</sub>O<sub>3</sub>, commercial sodium silicate solution (43%), NaOH (Merck), copper nitrate (Merck), NiSO<sub>4</sub>·7H<sub>2</sub>O (Merck), Commercial Rainy Nickel (Merck), Hydrazine hydrate

\* Corresponding author at: Physical Chemistry department, National Research Centre Dokki, El Behouth Street, Dokki, Cairo, Egypt.

E-mail address: [ehegazy77@yahoo.com](mailto:ehegazy77@yahoo.com) (E.Z. Hegazy).

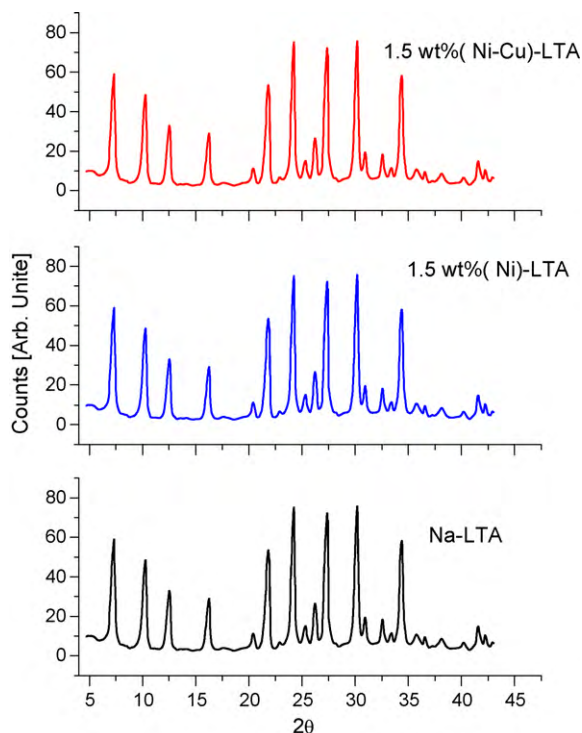


Fig. 1. XRD of Na-LTA and 1.5 wt% Ni-LTA and 1.5 wt% (1 Ni:1Cu)-LTA zeolites.

80% (Merck), *p*-nitrophenol (PNP) (Merck) and *p*-aminophenol (PAP) (as a standard materials), Ethanol (spectroscopic grade) (Merck).

## 2.2. Synthesis

Synthesis of zeolites was carried out by hydrothermal reaction of kaolin and commercial sodium silicate solution. LTA and FAU were obtained. The LTA is referring to Linde Type A zeolite and FAU is abbreviated to Faujasite type zeolite. For the ion exchange, 0.5 g of zeolite were dispersed in 100 ml of solutions of copper nitrate and nickel sulfate of different concentrations during continuous stirring at room temperature for 2 h. Reduction was done using hydrazine hydrate in an alkaline medium at 80–100 °C in order to obtain the metallic form of nickel.

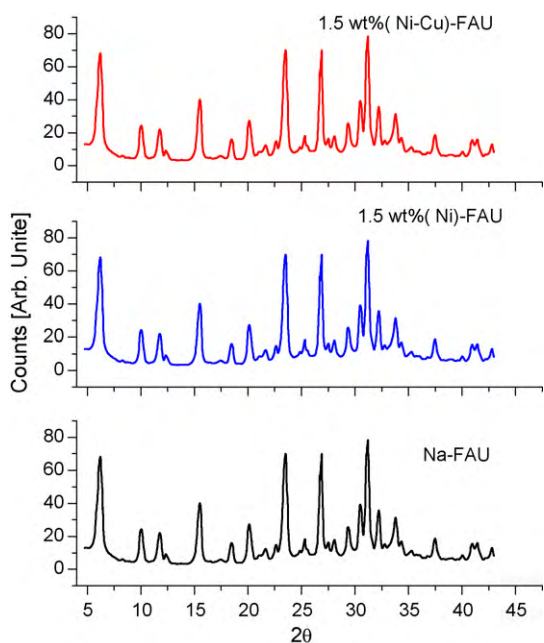


Fig. 2. XRD of Na-FAU and 1.5 wt% Ni-FAU and 1.5 wt% (1 Ni:1Cu)-FAU zeolites.

Table 1  
Crystal lattice parameters of different loaded zeolites.

Catalyst	Crystal system	Lattice constants		
		a	b	c
Na-LTA	Orthorhombic	12.3	8.3	4.3
0.1 wt% Ni-LTA	Orthorhombic	12.3	8.3	4.3
0.1 wt% (1Ni:1Cu)-LTA	Orthorhombic	12.3	8.3	4.3
0.5 wt% Ni-LTA	Orthorhombic	12.28	8.4	5.3
0.5 wt% (1Ni:1Cu)-LTA	Orthorhombic	12.25	8.6	5.5
1.5 wt% Ni-LTA	Orthorhombic	12.25	8.57	8.4
1.5 wt% (1Ni:1Cu)-LTA	Orthorhombic	12.25	8.57	8.4
Na-FAU	Orthorhombic	16.35	6.97	5.84
0.1 wt% Ni-FAU	Orthorhombic	16.28	6.96	5.83
0.1 wt% (1Ni:1Cu)-FAU	Orthorhombic	16.28	6.96	5.83
0.5 wt% Ni-FAU	Orthorhombic	12	8	6
0.5 wt% (1Ni:1Cu)-FAU	Orthorhombic	14.5	16	11
1.5 wt% Ni-FAU	Orthorhombic	10.1	9.69	6.38
1.5 wt% (1Ni:1Cu)-FAU	Triclinic $\alpha = 105$ , $\beta = 97.6$ , $\gamma = 90.75$	14.1	14.8	12.34

## 2.3. Hydrogenation process

Catalytic hydrogenation reaction was done by dissolving 0.1 mole of *p*-nitrophenol in an appropriate amount of ethanol (25 ml), followed by the addition of 10 ml hydrazine hydrate as hydrogen source, then heating at 80 °C. The catalyst was added to the heated solution and the time to reach 100% conversion was taken as a measure of the catalytic activity. The catalyst: reactant (PNP) was fixed at 1:5 molar ratio.

The filtrate was then taken and evaporated at reduced pressure and the residue was recrystallized from hot water to give pure product of PAP in almost 100% yield.

## 2.4. X-ray diffraction (XRD)

X-ray diffractograms of various solids were collected using Bruker D8 advance instrument with CuK $\alpha$ 1 target with secondly monochromator 40 kV, 40 mA.

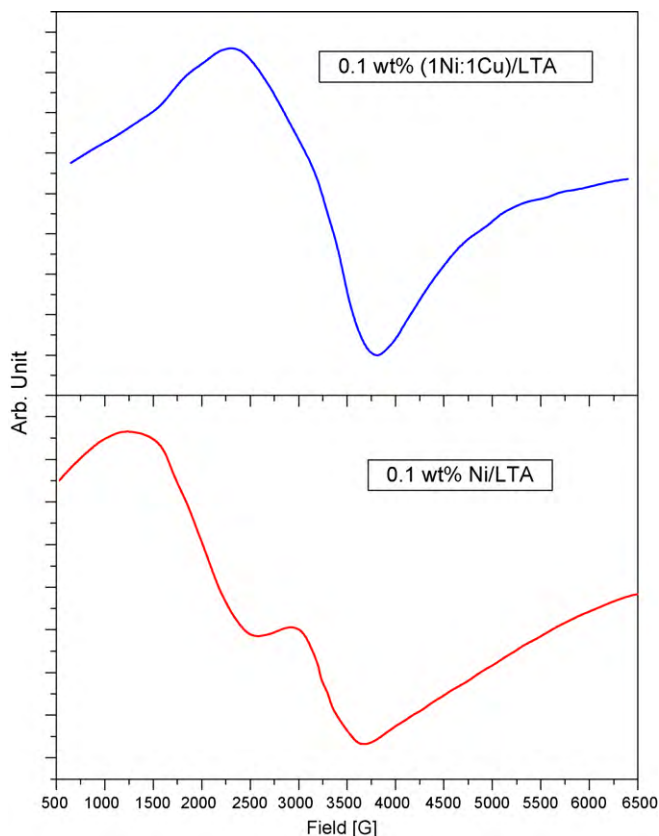


Fig. 3. ESR spectra of Ni and Ni:Cu-LTA zeolite.

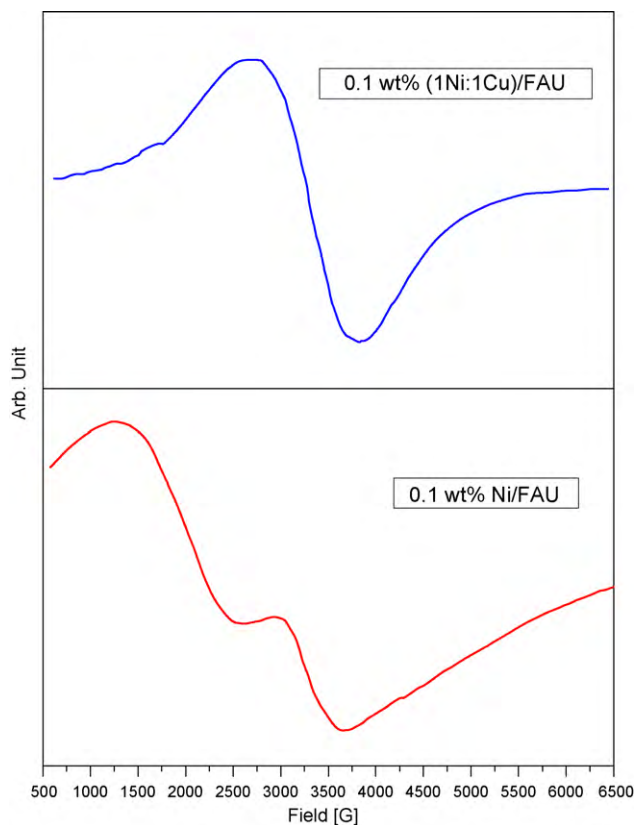


Fig. 4. ESR spectra of Ni and Ni:Cu-FAU zeolite.

### 2.5. ESR spectroscopy

ESR spectra of different solids were measured using (Bruker Elecsys. 500) operated at X-band frequency. The following parameters are generalized to all samples otherwise mentioned in the text. Microwave frequency: 9.73 GHz, receiver gain: 20, sweep width: 6000 center at 3480, microwave power: 0.00202637.

### 2.6. Transmission electron microscope (TEM)

Images of TEM was taken by instrument JTEM-1230, Japan, JEOL Company, 120 Kv Max, 0.2 nm resolution, 100 Kv operating voltage, CCD-camera option.

## 3. Results and discussion

### 3.1. XRD

X-ray diffractograms of bare zeolite and reduced single and bi-metal (1.5 wt%) loaded zeolites (LTA and FAU) are represented in Figs. 1 and 2. In these figures XRD diffractograms showed nearly no change in the degree of crystallinity which emphasis the idea that at these loadings the crystal structure and the porous system of zeolites LTA and FAU are not affected. In addition the crystallite size of metallic nickel is almost impossible to be determined from the diffraction lines of Ni because both zeolite LTA and FAU zeolites contain an overlapped diffraction lines at the same patterns of those of single metal and bimetal alloy.

In addition the crystal lattice parameters are calculated for the loading zeolites (Table 1). The results showed that in metal and bimetal loaded on LTA (up to 0.5 wt%) the lattice parameters suffered limited changes. The significant change could be observed only at high loading (1.5 wt%). However in case of FAU, the change is, however more pronounced even at 0.5 wt% and a considerable change occurs at 1.5 (Ni:Cu) – FAU sample where the crystal system is changed from orthorhombic to triclinic. This behavior of FAU indicates that the reduction of metal loaded on FAU affects mainly

**Table 2**  
Catalytic activity and ESR particle size of investigated samples.

Catalyst used	Time to reach 100% conversion (s), metal:PNP (1:5)	Particle size of Ni estimated from ESR spectrum (nm)
0.1 wt% Ni (LTA)	35	14.5
0.5 wt% Ni (LTA)	300	–
1.5 wt% Ni (LTA)	1000	–
0.1 wt% (1Ni:1Cu) (LTA)	15	14.7
0.1 wt% Ni (FAU)	103	–
0.5 wt% Ni (FAU)	225	–
1.5 wt% Ni (FAU)	360	–
0.1 wt% (1Ni:1Cu) (FAU)	43	13.0

the porous structure and may result in blocking of some of these pores which may be reflected in the catalytic activity as will be seen later.

### 3.2. ESR (electron spin resonance)

ESR spectroscopy is usually employed to characterize the paramagnetic centers where a free electron exists. In addition it attracts more interest when these particles diminished to a nanoscale.

Moreover, Kawabata [45] demonstrated his famous relation hypothesizing that the broadening of ESR signal of nanometal particles are suffering from quantum size effect and can be correlated to the size of the nanometal particle.

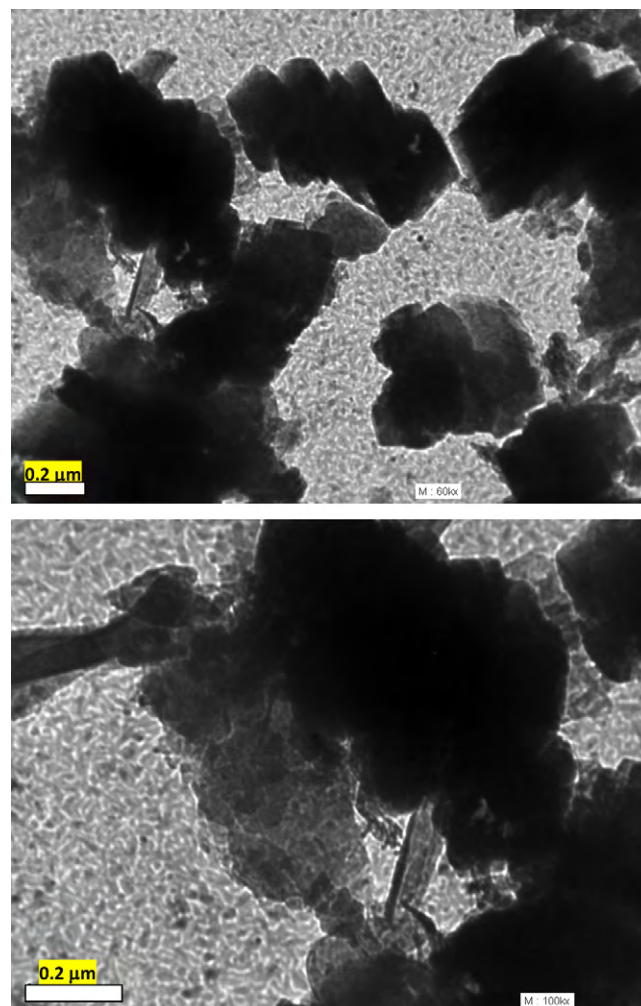


Fig. 5. TEM of 0.1 wt% Ni-LTA zeolite.

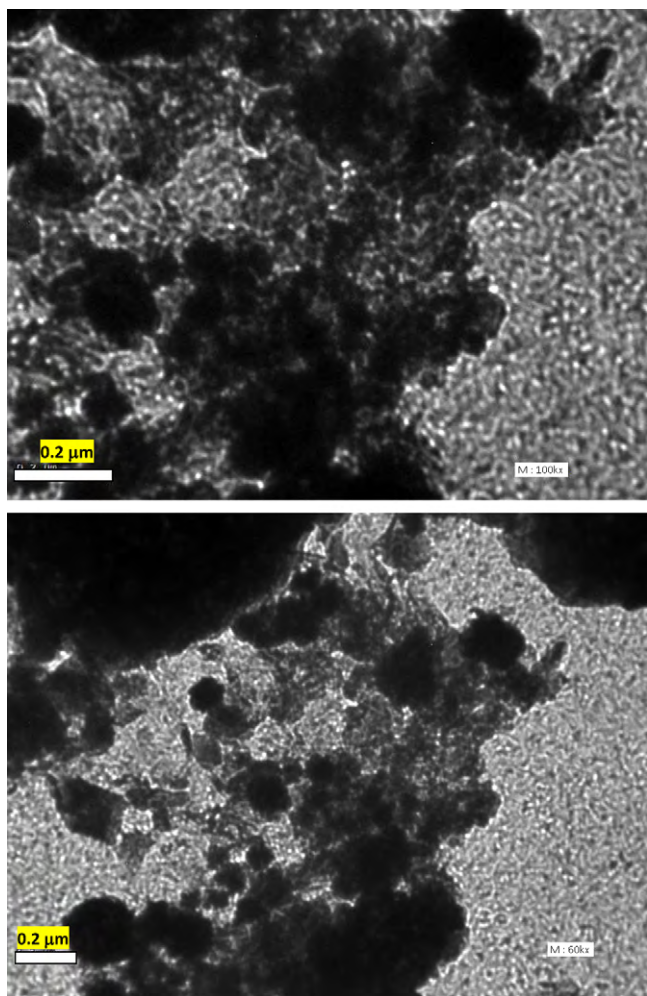


Fig. 6. TEM of 0.1 wt% (1Ni:1Cu)-LTA zeolite.

Accordingly, direct relationship between the line width  $\Delta H_{pp}$  (or peak to peak width) of the signal of nanoparticle in ESR spectra and its particle size are given in the following relation:

$$d = a(\Delta H_{pp})^{0.5} \quad (1)$$

where  $d$  is the particle size in nm,  $\Delta H_{pp}$  is the line width of ESR signal in mT and  $a$  is the proportionality constant.

The proportionality constant “ $a$ ” for our case nickel metal was found to be 1.2 [14]. This relation enables us to estimate precisely the average particle size of nickel even when not existing in crystalline form. The characteristic signal of nickel metal appeared at  $g=2.2$  [14]. The overlapping lower magnetic field signals were assumed to be attributed to the existence of strain between nanonickel particles [43,44].

The ESR spectra of high loading Ni-zeolite samples show highly anisotropy which indicates high strain among nanonickel particles (Fig. 3). Introducing the copper in this system to alloying the nickel with 1:1 mole ratio resulted in an observable decrease in this anisotropy which indicates that the formation of this alloy reduce more or less the high strain between nanonickel particles. An example of this behavior is given in Fig. 4 where 0.1 wt% Ni-FAU sample showed a remarkable anisotropy which disappears upon alloying with copper.

The particle size of some samples could be estimated by Kawabata equation (Table 2). However due to high anisotropy of the rest of samples the estimated particle size could not be performed.

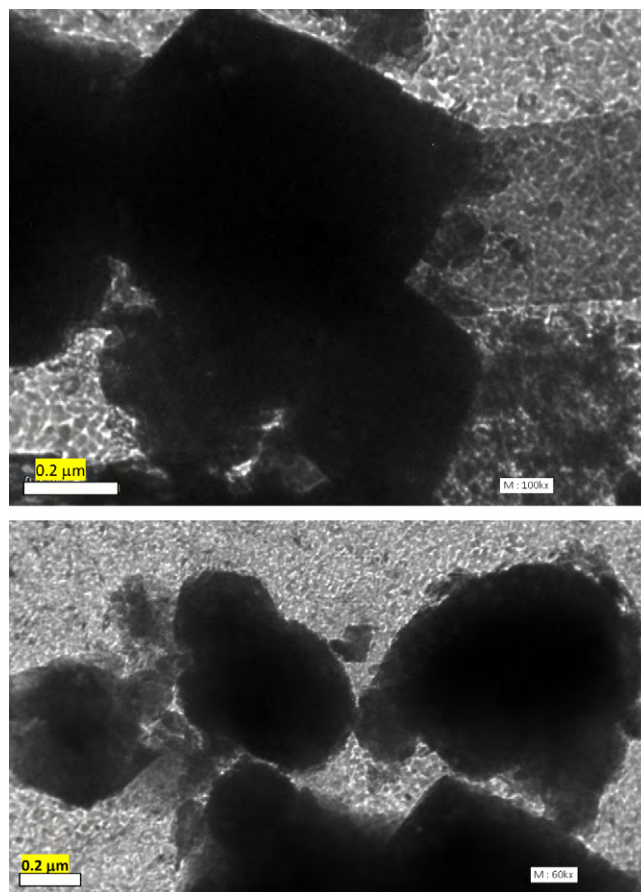


Fig. 7. TEM of 0.1 wt% (Ni)-FAU zeolite.

### 3.3. TEM (transmission electron microscope)

The TEM images of some selected samples are shown in Figs. 5–8.

Figs. 5 and 6 showed TEM of 0.1 wt% loading on LTA of both single Ni metal (Fig. 5) and bi metallic (1Ni:1Cu) (Fig. 6). Figs. 6 and 7 showed TEM of 0.1 wt% loading on FAU of both single Ni metal (Fig. 6) and bi metallic (1Ni:1Cu) (Fig. 7). From these images it could be easily observe that the alloying with copper increase the dispersion of metal on the surface of zeolite. The dispersion of metal on LTA zeolite was found to be higher than that of FAU zeolite.

### 3.4. Catalytic activity

The catalytic activity of different investigated samples were examined in the reaction of hydrogenation of *p*-nitrophenol into *p*-aminophenol using hydrazine hydrate as hydrogen donor as a model reaction. The mechanism of this reaction was assumed before in our previous work [43,44]. The time to reach 100% conversion is considered to be the best measure of the catalytic activity [43,44]. The results of catalytic activity of different samples under investigations are cited in Table 2.

From these results it is observed that the lower loading zeolites showed higher catalytic activity, i.e. as the amount of loading decrease the catalytic activity increase. This could be explained by assuming that the reactants here are  $H_2$  and *p*-nitrophenol which diffuse through the porous structure of each zeolite. And as the extent of loading increases these pores became more or less blocked thus opposing the reactants to diffuse through inner nickel metal particles. This decreasing the number of active centers with subsequent decrease in the catalytic activity. The catalytic activity of LTA

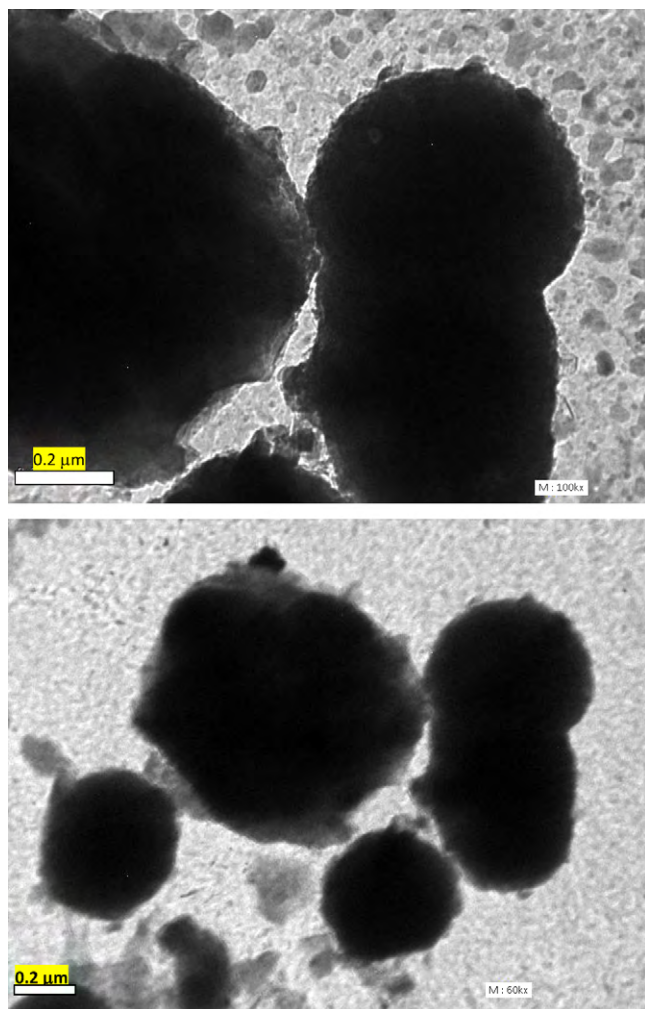


Fig. 8. TEM of 0.1 wt% (1Ni:1Cu)-FAU zeolite.

catalysts is being much higher than that of FAU catalysts especially at small extent of loading. This could be explained by the fact that the pore diameter of LTA is about 0.45 nm and that of FAU is 0.75 nm [13]. The smaller value of pore diameter of LTA with certain amount of loading diminishes the pore width to be optimum for hydrogen storage. The abnormal hydrogen absorption of 0.1 wt% LTA zeolite sample resulted in an increase of the concentration of H<sub>2</sub> in the vicinity of the pore of zeolite which increases the rate of the reaction that depends mainly on the hydrogen concentration. However by increasing the extent of loading to 0.5–1.5 wt% resulted in an amazing decrease in the catalytic activity which due to blocking of some of pores of LTA zeolite. This behavior is less observed for FAU catalysts which may be attributed to the larger volume of porous structure of FAU.

The bimetallic system (1Cu:1Ni) showed in all samples an increasing the catalytic activity expressed as a decrease in the time to reach 100% conversion. Keeping in mind that the single copper metal is not active in this hydrogenation process but it decomposes the hydrazine hydrate in the vicinity of highly active Ni metal in the same alloy resulted in increasing the amount of H<sub>2</sub> generated and hence increases the rate of the reaction.

#### 4. Conclusions

LTA and FAU could be used as an effective supports for Ni–Cu system for hydrogenation of *p*-nitrophenol. At lower loading

LTA zeolite exhibits hydrogen storage properties and increase the catalytic activity. The bimetallic (1Ni:1Cu) increases the catalytic activity with large extent. The Ni–Cu alloy decreases the Ni–Ni strain and increase dispersion of metal on zeolite. The very cheap raw materials from which zeolites were prepared (Egyptian kaolin) increase the economic impact of the use of such supports.

#### Acknowledgment

Authors are greatly appreciated to National Research Centre, Dokki, Cairo Egypt for Funding this research under the project title “Preparation and characterization of nanomaterials inside the nanocages of zeolite prepared from local materials and their uses as catalysts for synthesis of pharmaceutical & intermediate organic compounds and removal of wastes from water” No. 8030702.

#### References

- [1] H. Wu, D. Wexler, G. Wang, J. Alloys Compd. 488 (2009) 195.
- [2] H. Bi, K.-C. Kou, K.(K.) Ostrikov, Z.-C. Wang, J. Alloys Compd. 484 (2009) 863.
- [3] T. Hirano, T. Toshi, T. Watanabe, T. Akiyama, J. Alloys Compd. 470 (2009) 245.
- [4] J.L. Bobet, J. Huot, J.-G. Roquefere, S. Baduel, J. Alloys Compd. 469 (2009) 137.
- [5] Z.-Q. Zou, M. Meng, Y.-Q. Zha, J. Alloys Compd. 470 (2009) 96.
- [6] Y. Liu, J. Ma, J. Lai, Y. Liu, J. Alloys Compd. 488 (2009) 204.
- [7] K. Okada, J. Eur. Ceram. Soc. 28 (2008) 377.
- [8] M.A. Ermakova, D.Y. Ermakov, Appl. Catal. A (2003) 277.
- [9] J.L. Sebedio, G. Finke, R.G. Ackman, Chem. Phys. Lipids 34 (1984) 215.
- [10] S.M. Echeverria, V.M. Andres, Appl. Catal. 66 (1990) 73.
- [11] M.T. Rodrigo, L. Daza, S. Mendioroz, Appl. Catal. A 88 (1992) 101.
- [12] M.W. Balakos, E.E. Hernandez, Catal. Today 35 (1997) 415.
- [13] I.H. Abd El Maksoud, Preparation and regeneration of catalysts used in hydrogenation of edible oil, Ph.D. Thesis, Ain Shams University, 2005.
- [14] M.M. Selim, I.H. Abd El-Maksoud, Microporous Mesoporous Mater. 85 (2005) 273.
- [15] S. Farhadi, Z. Momeni, M. Taherimehr, J. Alloys Compd. 471 (2009) L5–L8.
- [16] U.B. Demirci, F. Garin, J. Alloys Compd. 463 (2008) 107.
- [17] A.C. Ferreira, A.M. Ferreira, A.M. Ferraria, A.M. Botelho do Rego, A.P. Gonçalves, M.R. Correia, T.A. Gasche, J.B. Branco, J. Alloys Compd. 489 (2010) 316.
- [18] L.J. Zhang, Z.Y. Wang, D.G. Xia, J. Alloys Compd. 426 (2006) 26.
- [19] H. Imamura, M. Suzuki, Y. Sakata, S. Tsuchiya, J. Alloys Compd. 303–304 (2000) 514.
- [20] Gurdip Singh, I.P.S. Kapoor, Shalini Dubey, J. Alloys Compd. 480 (2009) 270.
- [21] W.-B. Lee, K.-S. Bang, S.-B. Jung, J. Alloys Compd. 390 (2005) 212.
- [22] My.A. Boutbila, J. Rasneur, M. El Aatmani, J. Alloys Compd. 283 (1999) 88.
- [23] M. Sieben, M.M.E. Duarte, C.E. Mayer, J. Alloys Compd. 491 (2010) 722.
- [24] S.J. Naftel, A. Bzowski, T.K. Sham, J. Alloys Compd. 283 (1999) 5.
- [25] D. Phanon, K. Yvon, J. Alloys Compd. 490 (2010) 412.
- [26] Y. Kim, D. Reed, Y.-S. Lee, J.-H. Shim, H.-N. Han, D. Book, Y.W. Cho, J. Alloys Compd. 492 (2010) 597.
- [27] D.L. Croston, D.M. Grant, G.S. Walker, J. Alloys Compd. 492 (2010) 251.
- [28] Y. Zhu, W. Zhang, Z. Liu, L. Li, J. Alloys Compd. 492 (2010) 277.
- [29] E.A. Tereshina, A.V. Andreev, J. Kamarad, H. Drulis, J. Alloys Compd. 492 (2010) 1.
- [30] P.P. Hankare, B.V. Jadhav, K.M. Garadkar, P.A. Chate, I.S. Mulla, S.D. Delekar, J. Alloys Compd. 490 (2010) 228.
- [31] C.V. Rode, M.J. Vaidya, R. Jaganathan, R.V. Chaudhari, Chem. Eng. Sci. 56 (2001) 1299.
- [32] C.V. Rode, M.J. Vaidya, R.V. Chaudhari, Org. Process. Res. Dev. 3 (1999) 465.
- [33] T. Komatsu, T. Hirose, Appl. Catal. A: Gen. 276 (2004) 95.
- [34] S.S. Sathe, Process for preparing *p*-aminophenol in the presence of dimethyldodecylamine sulfate, US Patent 4,176,138 (1979).
- [35] L.T. Lee, M.H. Chen, C.N. Yao, Process for manufacturing *p*-aminophenol, US Patent 4,885,389 (1989).
- [36] K.S. Yun, B.W. Cho, Process for preparing paraaminophenol, US Patent 066,369 (1991).
- [37] M.J. Vaidya, S.M. Kulkarni, R.V. Chaudhari, Process. Res. Dev. 7 (2003) 202.
- [38] K. Venkatraman, The Chemistry of Synthetic Dyes, vol. I, Academic Press, New York, 1952, p. 184.
- [39] H.O. House, Modern Synthetic Reactions, 2nd ed., Benjamin, New York, 1977, p. 145.
- [40] P.N. Rylander, Hydrogenation Methods, Academic, New York, 1985, p. 365.
- [41] F.D. Popp, H.P. Schultz, Chem. Rev. 62 (1962) 19.
- [42] R.E. Harmon, S.K. Gupta, D.J. Brown, Chem. Rev. 72 (1972) 21.
- [43] I.H. Abd El Maksoud, T.S. Saleh, Green Chem. Lett. Rev. 3 (2) (2010) 127–134.
- [44] I.H. Abd El Maksoud, E.Z. Hegazy, S.H. Kenawy, T.S. Saleh, Adv. Synth. Catal. 352 (2010) 1169.
- [45] A. Kawabata, J. Phys. Soc. Jpn. 29 (1970) 902.